LANGMUIR

Article

pubs.acs.org/Langmuir

# Unusual Morphologies of Poly(vinyl alcohol) Thin Films Adsorbed on Poly(dimethylsiloxane) Substrates

Akchheta Karki,[†] Lien Nguyen,[†] Bhanushee Sharma, Yan Yan, and Wei Chen*

Chemistry Department, Mount Holyoke College, South Hadley, Massachusetts 01075, United States

Supporting Information

**ABSTRACT:** Adsorption of poly(vinyl alcohol) (PVOH), 99% and 88% hydrolyzed poly(vinyl acetate), to poly(dimethylsiloxane) (PDMS) substrates was studied. The substrates were prepared by covalently attaching linear PDMS polymers of 2, 9, 17, 49, and 116 kDa onto silicon wafers. As the PDMS molecular weight/thickness increases, the adsorbed PVOH thin films progressively transition from continuous to discontinuous morphologies, including honeycomb and fractal/droplet. The structures are the result of thin film dewetting that occurs upon exposure to air. The PVOH film thickness does not vary significantly on these PDMS substrates, implicating the PDMS thickness as the cause for the morphology differences. The adsorbed PVOH thin films are less stable and have a stronger tendency to dewet on thicker, more liquid-like PDMS layers. When $PVOH^{99\%}$ and $PVOH^{88\%}$ thin films are compared, fractal and droplet morphologies are observed on high molecular weight PDMS substrates, respectively. The formation of the unique fractal features in the $PVOH^{99\%}$ thin films as well as other crystalline and semicrystalline thin films is most likely driven by crystallization during the dehydration process in a diffusion-limited aggregation fashion. The only significant enhancement in hydrophilicity via PVOH adsorption was obtained on $PDMS^{2k}$, which is completely covered with a PVOH thin film. To mimic the lower receding contact angle and less liquid-like character of the $PDMS^{2k}$ substrate, light plasma treatment of the higher molecular weight PDMS substrates was carried out. On the treated PDMS substrates, the adsorbed PVOH thin films are in the more continuous honeycomb morphology, giving rise to significantly enhanced wettability. Furthermore, hydrophobic recovery of the hydrophilized PDMS substrates was not observed during a 1 week period. Thus, light plasma oxidation and subsequent PVOH adsorption can be utilized as a means to effectively hydrophilize conventional PDMS substrates. This study illustrates that the stability and morphology of adsorbed polymer thin films depend on polymer crystallinity as well as substrate physical properties.

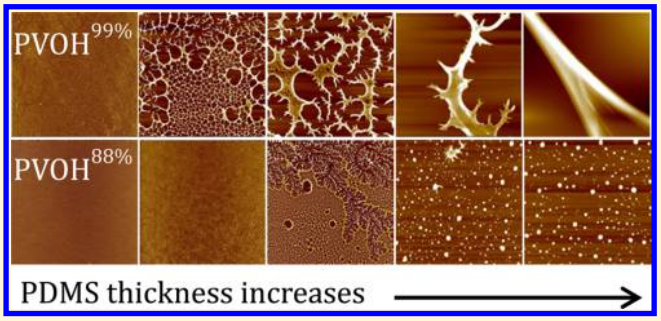


## INTRODUCTION

The ubiquity of silicones in science and technology can be attributed to their unique structural characteristics.[1−3] Poly(dimethylsiloxane) (PDMS), the most common type of silicone, is structurally distinct as shown in Figure 1. The Si−O and Si−C bonds are significantly longer than the carbon-based counterparts; the Si−O−Si bond angle is 143°, much larger than the typical bond angle of C−O−C. Furthermore, the electronegativity differences among Si, O, and C render the Si−O and Si−C bonds partially ionic, with Pauling percent ionic characters of 51% and 12%, respectively. These distinctive structural features of PDMS give rise to interesting physical and chemical properties. The vast conformational freedom of PDMS chains results in the low glass transition temperature of −123 °C for bulk PDMS.[4] PDMS is liquid at room temperature. Additionally, PDMS is highly oxygen- and water-vapor-permeable,[5] even though it is hydrophobic with a low surface tension of ∼20 mN/m.[4] Silicones are more thermally stable than their carbon-based polymers as the Si−O bond is stronger than C−C;[6] however, the ionic character of the Si−O bond renders silicones chemically reactive toward bases and acids.

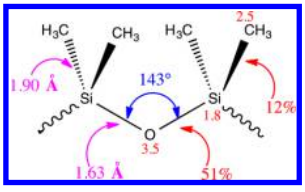


**Figure 1.** Unique structural features (bond length in pink, bond angle in blue, electronegativity and percent ionic character in red) of poly(dimethylsiloxane).

The unique characteristics of cross-linked PDMS, including elasticity, permeability, thermal stability, and reactivity, are taken advantage of in its applications.[2,3] Its hydrophobic nature, however, is often undesirable and manifests in poor wetting, weak adhesion, and nonspecific protein adsorption. A

**Received:** February 5, 2016
**Revised:** March 17, 2016
**Published:** March 22, 2016





DOI: 10.1021/acs.langmuir.6b00470
*Langmuir* 2016, 32, 3191−3198

significant effort has been directed at exploring methods to hydrophilize PDMS, ranging from plasma treatment to wet chemical approaches.[7,8] One method is the physical adsorption of poly(vinyl alcohol) (PVOH) from aqueous solution to functionalized PDMS.[9−12] All cited papers report that PVOH does not adsorb to native PDMS. This is substantiated by contact angle and infrared spectroscopy (IR) analyses; however, neither atomic force microscopy (AFM) images nor ellipsometric thickness data were reported. This is perplexing because PVOH adsorption was established as a general method to hydrophilize hydrophobic substrates more than a decade ago.[13−16] PVOH is different from other water-soluble synthetic polymers in that it is atactic yet crystalline. In previous studies, adsorption was carried out on a variety of polymeric substrates and monolayers supported on silicon wafers with different chemical compositions and surface energies. The only two substrates that PVOH did not adsorb to were clean silicon wafers and poly(ethylene glycol) monolayers.[15] Extensive PVOH adsorption on polystyrene[17] and gold[18] substrates has also been reported. The spontaneous PVOH adsorption was attributed to "hydrophobic interactions," or the release of water molecules from the solid−liquid interface, and the subsequent crystallization of PVOH polymer chains at the interface.[15] Crystallinity in PVOH stems from double hydrogen bonds of hydroxyl groups in each monoclinic unit cell.[19] IR and electron diffraction data validated the crystalline nature of the adsorbed PVOH on certain substrates.[15] The PVOH thin films adsorbed on the prepared hydrophobic substrates are smooth and continuous by AFM with reproducible ellipsometric thicknesses (2.6 ± 0.2 nm for PVOH of 89−98 kDa and 99% hydrolyzed).[15] High PVOH concentrations, high solution ionic strengths, or significantly higher adsorption temperatures than room temperature can give rise to nonuniform films due to chain entanglement, aggregation, and lower polymer solubility.[16]

Although continuous PVOH thin films were produced in previous studies, discontinuous or dewetted polymer thin films are often observed in different systems as the result of free energy minimization. Thin film dewetting has been reviewed in the literature and can be taken advantage of in surface patterning.[20−22] Mechanisms of dewetting include "spinodal dewetting" for unstable thin films below a capillary length-determined thickness, "heterogeneous nucleation" by surface defects for thicker, metastable thin films, and "thermal nucleation" or "homogeneous nucleation" by thermal activation for metastable thin films.[20] The initially generated holes can continue to grow, merge, and rupture, resulting in honeycombs, ribbons, and/or droplets.[23]

Fractal or dendritic feature is another type of discontinuous morphology. Fractal structure is repeated in multiple length scales, very often in a statistical, nonexact fashion. There has been a significant amount of theoretical work on modeling fractal structures. In the early 1980s, Witten and Sanders proposed the "diffusion-limited aggregation" (DLA) model, which assumes that the kinetic growth of clusters involving random-walk diffusion and irreversible addition of new particles to the edges of the existing, immobile structures with diffusion being the rate-limiting step.[24,25] The highly dendritic nature of fractal morphology is the result of the exposed ends being more prone to new particle addition than the sites near the center of the cluster. Fractal structures in topographical dimensions of two and higher have been studied using the DLA model.[26] Thin films with fractal morphology have been prepared experimentally. For example, metal oxide nanoparticles,[27] blends containing polyaniline or its oligomeric counterpart,[28] polyelectrolyte containing sodium chloride salt,[29] poly(ethylene glycol),[30,31] stereoregular poly(methyl methacrylate),[32] and isotactic polystyrene,[33] form fractal-type structures upon spin-casting from their solutions on flat substrates. Upon further examination, the materials that formed fractal features in these studies are either crystalline or semicrystalline. These reports did point out that fractal structure formation is driven by crystallization forces and follows the DLA model.[27−33] Most of the reported sample preparations, however, involved spin-casting. There is one report describing fractal structure formation of type I collagen adsorbed on polystyrene after a slow drying process.[34] As the adsorbed amount of collagen increased, its morphologies evolved from dendritic to honeycomb-like to continuous based on AFM analysis.[34] On the other hand, the morphologies of the adsorbed collagen films appear continuous after fast drying.[34] The formation of the discontinuous morphologies was attributed to dewetting; however, crystallization was not mentioned in the study. It is likely that crystallization of collagen is allowed to take place to a greater extent in the slower drying process, which contributes to the fractal structure formation. On the basis of the existing literature work, it appears that fractal morphology formation of a thin film on a solid support requires dewetting of the thin film as well as crystallization of a component material in the thin film during the drying process.

In this work, we investigated PVOH adsorption to PDMS substrates from aqueous solution and the morphologies of PVOH thin films upon drying. We chose nanoscopically thin PDMS layers supported on silicon wafers instead of bulk PDMS to allow systematic variation of PDMS layer thickness as well as characterization by ellipsometry and AFM. Two types of PVOH polymers with similar molecular weight and different degrees of hydrolysis, namely, 99% and 88%, were selected to discern the effect of PVOH crystallinity on film morphology. We find that PVOH spontaneously adsorbs to PDMS substrates to a similar extent as to other hydrophobic substrates. However, the exhibited PVOH morphologies vary from continuous films to various discontinuous morphologies including fractals, honeycombs, and droplets on different length scales. The discontinuous morphologies are attributed to the instability of the adsorbed PVOH thin films on liquid-like PDMS layers. Fractal morphologies were only observed in the 99% hydrolyzed PVOH system, and we attribute this to the crystallization of PVOH chains during film dehydration in a DLA fashion. Light plasma oxidation of PDMS substrates results in significantly reduced PVOH dewetting and enhanced hydrophilicity. Hydrophilized PDMS samples with complete or incomplete PVOH coverage did not undergo hydrophobic recovery for at least 1 week. In this study, we demonstrated that stability and morphology of adsorbed polymer thin films depend on polymer crystallinity as well as substrate physical properties for the first time to the best of our knowledge. The findings of this study also provide a practical solution to permanently hydrophilize silicones.

## MATERIALS AND METHODS

**Materials.** Silicon wafers (100 orientation, P/B doped, resistivity 1−10 Ω·cm, thickness 475−575 μm) were purchased from International Wafer Service. Silicon-coated (15−30 nm) TEM copper grids were obtained from Electron Microscopy Sciences. Trimethylsiloxy-terminated poly(dimethylsiloxanes)


DOI: 10.1021/acs.langmuir.6b00470
Langmuir 2016, 32, 3191−3198

(PDMS$^{2k}$, MW = 2 kDa; PDMS$^{9k}$, MW = 9 kDa; PDMS$^{17k}$, MW = 17 kDa; PDMS$^{49k}$, MW = 49 kDa; PDMS$^{116k}$, MW = 116 kDa) were purchased from Gelest. Poly(vinyl alcohol) polymers (PVOH$^{99\%}$, MW = 89−98 kDa and 99+% hydrolyzed; PVOH$^{88\%}$, MW = 85−124 kDa and 88% hydrolyzed) were purchased from Sigma-Aldrich. HPLC-grade organic solvents were obtained from Pharmco. Oxygen gas (99.999%) was purchased from Middlesex Gases Technologies. Water was purified using a Millipore Milli-Q Biocel System (Millipore Corp., resistivity ≥18.2 MΩ/cm). All reagents were used as received without further purification. Glassware was cleaned in a base bath (potassium hydroxide in isopropyl alcohol and water), thoroughly rinsed with distilled water, and stored in a clean oven at 110 °C until use.

**Instrumentation.** Silicon wafers were oxidized in a PDC-001 Harrick plasma cleaner. Dynamic light scattering (DLS) measurements were carried out using a Malvern Zetasizer Nano-S equipped with a 4 mW He−Ne laser ($\lambda$ = 632.8 nm) to determine the size of PVOH chains in solution. Refractive indices of PVOH ($n$ = 1.520) and water ($n$ = 1.330) and viscosity of water ($\eta$ = 0.8872) at 25 °C were assigned. Contact angle was measured using a Ramé-Hart telescopic goniometer with a Gilmont syringe and a 24-gauge flat-tipped needle. Dynamic advancing ($\theta_A$) and receding ($\theta_R$) angles were captured by a camera and digitally analyzed while Milli-Q water in the syringe was added to and withdrawn from the drop, respectively. The standard deviation of the reported contact angle values is less than or equal to 2° unless specified otherwise. Native silicon dioxide and polymer layer thicknesses were measured using a Gaertner Scientific LSE Stokes ellipsometer at a 70° incident angle (from the normal to the plane). The light source is a He−Ne laser ($\lambda$ = 632.8 nm). Thickness was calculated using the following refractive indices: air, $n_o$ = 1; silicon oxide and polymer layers, $n_1$ = 1.46; silicon substrate, $n_s$ = 3.85, and $k_s$ = −0.02 (absorption coefficient). Measurement error is within 1 Å as specified by the manufacturer. Each reported thickness and contact angle value is an average of at least 16 measurements obtained from at least four samples from two different batches and four readings from different locations on each sample. In situ imaging of PVOH adsorption on PDMS substrates and desorption of PVOH adsorbed on PDMS substrates was carried out using a Nikon water immersion lens (10×) and a QICAM Q-Imaging camera attached to a Nikon eclipse 50i optical microscope. An Olympus BX51 optical microscope in the reflective mode was used to obtain microscopic images of substrates. Nanoscopic surface topography was imaged using a Veeco Metrology Dimension 3100 atomic force microscope (AFM) with a silicon tip operating in tapping mode. Roughness and section analyses of surface features were determined using Nanoscope software. Multiple optical and AFM images from different samples of the same type and different locations on each sample were captured; representative images are presented and variations are noted in the text. Electron diffraction studies were carried out using a FEI Tecnai 12 transmission electron microscope (TEM) at 120 kV.

**Preparation of PDMS Substrates.** PDMS polymers were covalently attached to silicon wafers following a literature procedure.[35] Silicon wafers were diced into 1.2 × 1.5 cm$^2$ pieces, rinsed thoroughly with distilled water, dried with compressed air, and further dried in a clean oven at 110 °C for 30 min prior to being exposed to oxygen plasma at ∼300 mTorr for 15 min at high power (30 W). An amount of 100 μL of PDMS polymer was dispensed on each clean wafer using a micropipette. Samples were then heated to 100 °C for 24 h in capped scintillation vials. After the reaction, the wafers were rinsed individually with toluene (3×), acetone (3×), and Milli-Q water (3×), and dried under a nitrogen stream to remove excess water and in a desiccator overnight.

**Adsorption of PVOH onto PDMS Substrates.** The 0.1 wt % PVOH solutions were prepared by dissolving 0.1 g of PVOH powder in 100 g of Milli-Q water at 88−94 °C for 3 h under stirring in a clean 120 mL polypropylene bottle. The resulting solution was allowed to cool overnight while being stirred. DLS was used to monitor the size distribution and aggregation state of PVOH chains over time. An additional 3−4 days of equilibration at room temperature without stirring was found necessary for the PVOH chains to reach their equilibrium conformation. The PVOH solutions were used within 30 days before polymer aggregation takes place. For the adsorption studies, PDMS substrates were submerged in 15 mL of PVOH solution at room temperature for 24 h. Out of concern that some Langmuir−Blodgett-like deposition might occur when samples were removed through the solution−air interface, the solution was diluted with water a total of six times before removing the samples. For each dilution, 30 mL of Milli-Q water was added to the solution and the mixture was stirred for 1 min, after which 30 mL of solution was removed within 1 min. After removing the samples from water, excess water was gently removed by touching the edge of each sample with the bottom of a dry Petri dish. The samples were dried in a desiccator overnight. Stability tests of the adsorbed PVOH layers were carried out by immersing the samples in Milli-Q water at room temperature for 24 h. Identical dilution and drying protocols were followed prior to sample characterization.

**In Situ Optical Microscopy Imaging.** A sample was fixed to the bottom of a polypropylene Petri dish, which was then filled with either PVOH solution (filtered using a 0.2 μm Nylon filter) or Milli-Q water to ∼90% full. A water-immersion lens was dipped into the solution through a hole in the cover of the dish. Time-lapse images of the sample surface were captured every hour for a total duration of 23 h.

## RESULTS AND DISCUSSION

**PDMS Substrates.** Covalently attached PDMS thin layers on silicon substrates were prepared according to a reported procedure.[35] Ellipsometric thickness, AFM root-mean-square (rms) roughness, and dynamic water contact angles of the PDMS layers are summarized in Table 1. The thickness values are consistent with those in the literature,[35] and are further correlated with the PDMS molecular weights shown in Figure

**Table 1. Characterization of Covalently Attached PDMS Layers of Different Molecular Weights: Thickness, Roughness (AFM Image Size, 2.5 × 2.5 μm$^2$), and Advancing and Receding Water Contact Angles ($\theta_A/\theta_R$)**

| PDMS MW (kDa) | thickness (nm) | rms roughness (nm) | $\theta_A/\theta_R$ (deg) |
|---|---|---|---|
| 2 | 1.2 ± 0.2 | 0.2 | 101 ± 2/79 ± 3 |
| 9 | 3.6 ± 0.4 | 0.3 | 107 ± 2/102 ± 2 |
| 17 | 4.4 ± 0.4 | 0.3 | 109 ± 2/104 ± 2 |
| 49 | 7.6 ± 0.5 | 0.4 | 109 ± 2/95 ± 2 |
| 116 | 11.3 ± 0.7 | 0.5 | 113 ± 2/98 ± 2 |



DOI: 10.1021/acs.langmuir.6b00470
Langmuir 2016, 32, 3191−3198

2. A strong power law relationship, thickness = $k(MW)^{0.57}$, indicates that the thickness of the grafted PDMS chains is

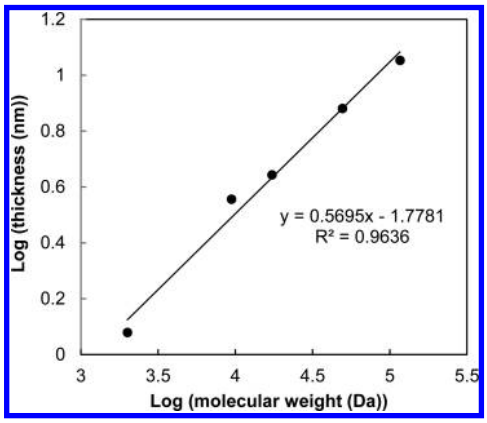


**Figure 2.** PDMS layer thickness as a function of PDMS molecular weight shows a strong power law relationship with the exponent equal to 0.57.

correlated to the polymer's original molecular weight even though chain scissions likely take place during the attachment process.[35]

AFM images of the PDMS layers shown in Figure 3 appear rougher as the PDMS molecular weight increases. This trend is

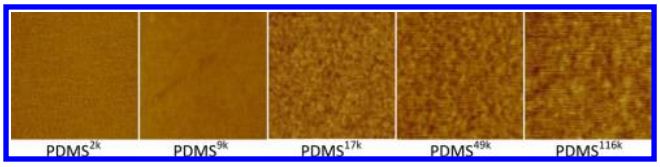


**Figure 3.** AFM Images (size, 2.5 × 2.5 $\mu m^2$; height scale, 10 nm) of the PDMS substrates.

substantiated by the rms roughness values in Table 1. Furthermore, wettability of these layers, given in the last column in Table 1, indicates that the grafted PDMS layers are hydrophobic with their respective advancing and receding contact angles similar to those of micrometer-thick, spin-cast PDMS films, 117° ± 8° and 104° ± 4°.[36] The contact angles of the $PDMS^{2k}$ surface, especially the receding contact angle, however, are somewhat lower, implying that the surface coverage by the PDMS chains is less than complete and/or more Si−OH chain ends are exposed at the interface. For these reasons, 2 kDa is the lowest molecular weight of PDMS evaluated in this study. The $PDMS^{9k}$ and $PDMS^{17k}$ substrates have higher contact angles, indicating more complete surface coverage by the PDMS polymer. When the PDMS molecular weight increases further to 49 and 116 kDa, contact angle hysteresis (difference between advancing and receding angles) rises noticeably, most likely due to increased surface roughness. The prepared PDMS layers range from 1.2 to 11.3 nm in thickness with increasing surface roughness. Except for $PDMS^{2k}$, the grafted PDMS layers are similar in hydrophobicity as conventional PDMS substrates.

**Morphologies and Formation Mechanism of Adsorbed PVOH Thin Films.** Adsorption of $PVOH^{99\%}$ to the PDMS substrates from dilute aqueous solution was carried out as described in the Materials and Methods section. Optical micrographs and AFM images of the $PVOH^{99\%}$−PDMS surfaces are shown in Figure 4. The morphological differences

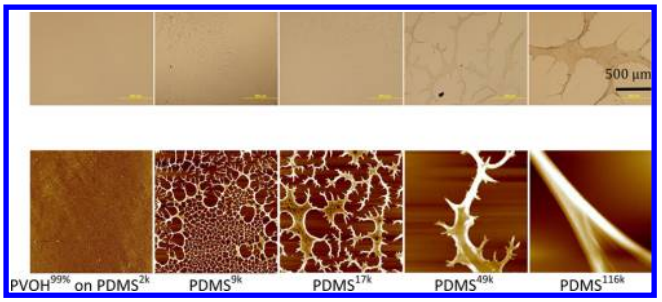


**Figure 4.** Optical micrographs (scale bar, 500 $\mu m$) and AFM images (size, 20 × 20 $\mu m^2$; height scales, 20, 30, 40, 100, and 400 nm from left to right) of $PVOH^{99\%}$ thin films adsorbed on PDMS substrates.

of the adsorbed $PVOH^{99\%}$ thin films on different PDMS substrates are significant and reproducible. On $PDMS^{2k}$, $PVOH^{99\%}$ thin films are smooth and continuous at both microscopic and nanoscopic levels. As the PDMS molecular weight/thickness increases, the $PVOH^{99\%}$ thin films become progressively discontinuous and larger, sparser fractal features are formed. We note that both honeycomb and continuous morphologies are present on $PDMS^{2k}$ and that other mixed morphologies are observed on $PDMS^{9k}$ and $PDMS^{17k}$. The AFM images of $PVOH^{99\%}$−$PDMS^{9k}$ and $PVOH^{99\%}$−$PDMS^{17k}$ capture regions where honeycomb and fractal morphologies coexist with the former being dominant on $PVOH^{99\%}$−$PDMS^{9k}$ and the latter being the main feature on $PVOH^{99\%}$−$PDMS^{17k}$.

In situ optical microscopy imaging was carried out to elucidate the formation mechanism of the discontinuous morphologies, i.e., whether the features are formed in situ in solution or ex situ upon drying. Time-lapse images of the $PDMS^{2k}$ (used as a control) and $PDMS^{49k}$ substrates submerged in a $PVOH^{99\%}$ solution were captured every hour for 23 h and are shown in the Supporting Information (Figures 1S and 2S). Both the $PVOH^{99\%}$−$PDMS^{2k}$ and $PVOH^{99\%}$−$PDMS^{49k}$ surfaces remain smooth and featureless during the time-lapse experiment. However, as soon as the $PVOH^{99\%}$−$PDMS^{49k}$ sample was removed from the solution, its surface became visibly cloudy and fractal morphologies were observed using both optical microscopy and AFM. The in situ imaging study illustrates that the discontinuous morphologies are formed by dewetting during the drying process and are likely the result of dehydration-caused instability of the $PVOH^{99\%}$ thin films. As to why the nature of the substrate dramatically influences the extent of dewetting, we hypothesize that the adsorbed PVOH thin films become progressively unstable as the underlying PDMS layers become thicker and increasingly manifest the liquid-like characteristic of bulk PDMS. Furthermore, the AFM images of the PDMS substrates reveal enhanced surface roughness as the PDMS thickness increases. A higher density of surface defects can likely contribute to a greater extent of dewetting by "heterogeneous nucleation". Lastly, the $PDMS^{2k}$ substrate not only has the thinnest PDMS layer but also exhibits an unusually low receding contact angle, which can pin the PVOH thin films and prevent them from dewetting, resulting in the only continuous $PVOH^{99\%}$ thin films observed on any PDMS substrate. Whether it is PDMS thickness, surface roughness/defects, receding contact angle, or a combination of these factors, PDMS substrates cause the adsorbed $PVOH^{99\%}$ thin films to dewet to different extents and exhibit a variety of morphologies.

The progressive transition of the $PVOH^{99\%}$ thin films from continuous to honeycomb to fractal morphologies is similar to



DOI: 10.1021/acs.langmuir.6b00470
Langmuir 2016, 32, 3191−3198

that of the type I collagen thin films adsorbed on polystyrene after a slow drying process.[34] The main difference is that the cause of the transition is the nature of the substrate in our study and the adsorbed amount in the reported work. When the adsorbed amount of collagen was high, the films were stable and remained continuous upon dehydration. On the other hand, when the adsorbed amount was lower, the collagen films were too thin to be stable so that they broke up into honeycomb-like structures at the intermediate adsorbed amount and fractal features at the lowest adsorbed amount. Regardless of the cause, continuous, honeycomb, and fractal morphologies represent a progressive decrease in stability of the adsorbed thin films.

Adsorption of PVOH$^{88\%}$ onto the PDMS substrates was also carried out to probe the effect of PVOH degree of hydrolysis. Optical micrographs and AFM images of the resulting samples are presented in Figure 5. Similar to the PVOH$^{99\%}$–PDMS

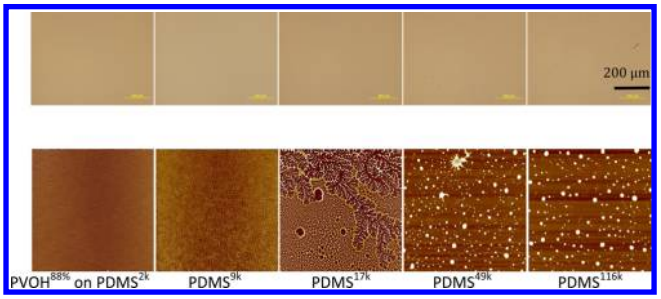


**Figure 5.** Optical micrographs (scale bar, 200 $\mu$m) and AFM images (size, 20 × 20 $\mu$m$^2$; height scales, 20, 20, 30, 100, and 100 nm from left to right) of PVOH$^{88\%}$ thin films adsorbed on PDMS substrates.

surfaces, PVOH$^{88\%}$ thin films are smooth and continuous on PDMS$^{2k}$ and become increasingly discontinuous as the PDMS layers become thicker, transitioning into honeycombs and specks. Mixed morphologies also frequently coexist on the PDMS substrates of intermediate molecular weights. This indicates that the PDMS substrates have similar effects on the (in)stability of both types of PVOH thin films. However, this is the only similarity between the PVOH$^{99\%}$ and PVOH$^{88\%}$ thin films. On the microscopic level, all PVOH$^{88\%}$ thin films are smooth except that fine, compact, branchlike features are discernible on PVOH$^{88\%}$–PDMS$^{116k}$ under high magnification. Although fractal morphology was observed occasionally, for example, in a mixed morphology region shown in the AFM image of PVOH$^{88\%}$–PDMS$^{17k}$, it is mostly absent in the PVOH$^{88\%}$ thin films.

It is suspected that the significant morphology differences between the PVOH$^{99\%}$ and PVOH$^{88\%}$ thin films are due to difference in polymer crystallinity. Electron diffraction studies were carried out on PVOH–PDMS$^{2k}$ samples supported on silicon-coated TEM grids to probe the crystallinity of the adsorbed PVOH polymers. The PVOH$^{99\%}$ thin film shows strong electron diffractions from the crystalline domains with the characteristic (200), (110), and (010) crystal planes indicated, while the PVOH$^{88\%}$ sample exhibits mostly amorphous halo with a few weak diffraction spots (Figure 6). It should be noted that electron diffraction studies were carried out in thicker regions of the samples where polymer adsorption takes place three dimensionally since the smooth regions were too thin to generate diffraction patterns. Figure 3S shows the regions where the electron diffractions were obtained.

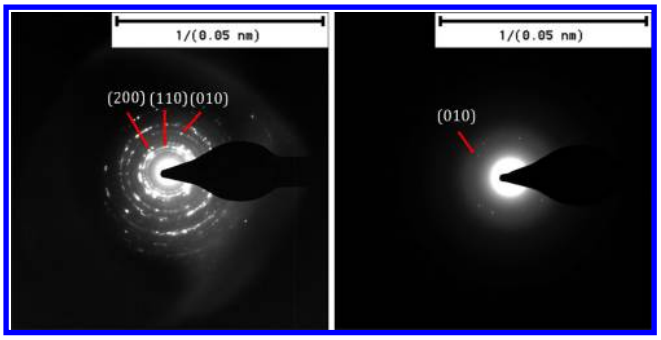


**Figure 6.** Electron diffraction patterns of PVOH$^{99\%}$ (left) and PVOH$^{88\%}$ (right) thin films adsorbed on PDMS$^{2k}$ substrates supported on silicon-coated TEM copper grids. PVOH has a monoclinic unit cell consisting of two molecules with lattice parameters of $a$ = 0.781 nm, $b$ = 0.252 nm, $c$ = 0.551 nm, and $\beta$ = 91°42′ (ref 19).

The electron diffraction results imply that crystallization of PVOH$^{99\%}$ in a diffusion-limited aggregation fashion during the drying process gives rise to the fractal features, similar to those consisting of collagen and other crystalline or semicrystalline materials reported in the literature.[27−34] On the other hand, the crystallization driving force is not as prominent during the drying of the PVOH$^{88\%}$ thin films. As the result, PVOH$^{88\%}$ thin films break up to form the more typical droplets. Our data, along with those reported in the literature, point to crystallization as a necessary criterion for the formation of fractal features.

**Other Characteristics of the PVOH Thin Films.** Adsorbed PVOH$^{99\%}$ and PVOH$^{88\%}$ thin films are further compared in thickness and surface wettability, as shown in Figure 7. As the PDMS molecular weight increases, the PVOH

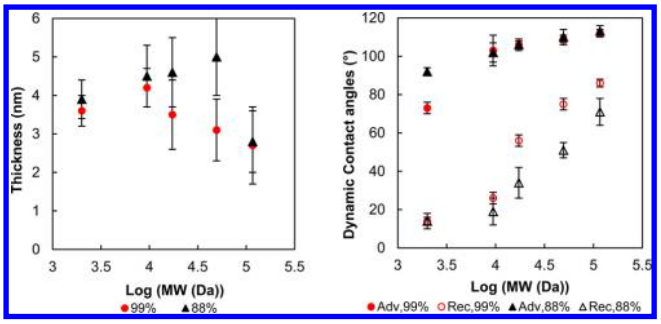


**Figure 7.** Thickness (left) and advancing and receding water contact angles (right) of PVOH$^{99\%}$ and PVOH$^{88\%}$ thin films adsorbed on PDMS substrates as a function of PDMS molecular weight.

film thickness shows a small, initial increase and a more noticeable, final decrease. The enhanced hydrophobic driving force on the more hydrophobic PDMS$^{9k}$ relative to PDMS$^{2k}$ and the reduced PVOH adsorption on the thicker, more liquid-like PDMS substrates are the likely causes for the initial rise and the final drop in the adsorbed amount, respectively. We note that the standard deviation of the film thickness is significant, especially for discontinuous, heterogeneous films. The trends mentioned above are not pronounced when taking the large standard deviation into consideration. The average thickness of PVOH$^{99\%}$ thin films is ∼3 nm and that of PVOH$^{88\%}$ thin films is ∼4 nm with the latter being slightly thicker due to the more disordered polymer conformation of the adsorbed PVOH$^{88\%}$; this is consistent with the earlier report.[16]



DOI: 10.1021/acs.langmuir.6b00470
Langmuir 2016, 32, 3191−3198

When the PVOH thin films become more discontinuous, advancing contact angles of the films approach that of the exposed hydrophobic PDMS substrate, and the receding contact angles increase more drastically as the surface coverage by PVOH decreases. There is a noticeable difference between the receding contact angles of $PVOH^{99\%}$ and $PVOH^{88\%}$ films. The higher surface coverage by $PVOH^{88\%}$, as shown by the optical micrographs (Figures 4 and 5), causes the $PVOH^{88\%}$ films to have lower receding contact angles. In a control experiment, the dynamic contact angles on ~1 mm thick Sylgard-184 films were 112° ± 6°/79° ± 6° after adsorption with $PVOH^{99\%}$, similar to those on PVOH−$PDMS^{116k}$. On the basis of the data obtained in this study, the insignificant decrease in water contact angles after PVOH adsorption on native PDMS substrates reported in literature is most likely due to the low coverage of dewetted PVOH thin films on thick, liquid-like PDMS substrates. Much lower advancing and receding contact angles are achieved when continuous films of $PVOH^{99\%}$ and $PVOH^{88\%}$ are obtained on the $PDMS^{2k}$ substrate, resulting in contact angles of 73° ± 3°/14° ± 2° and 92° ± 2°/14° ± 4°, respectively. The larger acetate content in the $PVOH^{88\%}$ films contributes to the higher advancing contact angle. The contact angles of $PVOH^{99\%}$−$PDMS^{2k}$ are pretty similar to those of $PVOH^{99\%}$ adsorbed on other hydrophobic substrates.[15,16] On the basis of these results obtained, the adsorbed PVOH thin films need be continuous to provide effective improvement in hydrophilicity for PDMS substrates.

The stability of the PVOH films was evaluated by immersing $PVOH^{99\%}$−$PDMS^{2k}$, $PVOH^{88\%}$−$PDMS^{2k}$, $PVOH^{99\%}$−$PDMS^{49k}$, and $PVOH^{88\%}$−$PDMS^{49k}$ in water for 24 h at room temperature. In situ imaging analyses of the samples reveal that the PVOH morphologies are conserved (Figure 4S), with a slight decrease in feature size noticeable in certain regions (not shown here). On average, $PVOH^{99\%}$ and $PVOH^{88\%}$ thin films decreased by ~10% and 30−40% in thickness, respectively. The stability difference can be attributed to the higher degree of crystallinity of $PVOH^{99\%}$. There is little distinguishable difference in stability between the continuous PVOH films on $PDMS^{2k}$ and the discontinuous films on $PDMS^{49k}$. Strategies such as cross-linking PVOH chains using glutaldehyde[15] can be used to improve their stability for long-term applications.

One of the main goals of this research is to use PVOH adsorption as a means to hydrophilize PDMS substrates. During the course of this endeavor, we recognized that the most significant wettability improvement was accomplished when the PDMS substrates were completely covered by continuous PVOH thin films. $PDMS^{2k}$ is the only substrate on which adsorbed PVOH thin films do not dewet and break up into discontinuous morphologies. In the earlier discussion, we attributed this to the substrate's lower receding contact angle, lower density of surface defects, and/or less liquid-like behavior. In an attempt to test these hypotheses and to prepare continuous PVOH thin films on other PDMS substrates, $PDMS^{49k}$ and $PDMS^{116k}$ substrates were lightly oxidized by exposure to oxygen plasma for 1 s prior to PVOH adsorption to introduce receding contact-line pinning sites. Figure 8 shows the AFM images of $PVOH^{99\%}$ and $PVOH^{88\%}$ thin films adsorbed on $PDMS^{49k}$ substrates before and after oxygen plasma treatment. Apparently, the short-time plasma treatment has a considerable effect on the PVOH morphology. The dynamic contact angles of the treated $PDMS^{49k}$ are 101°/80°,

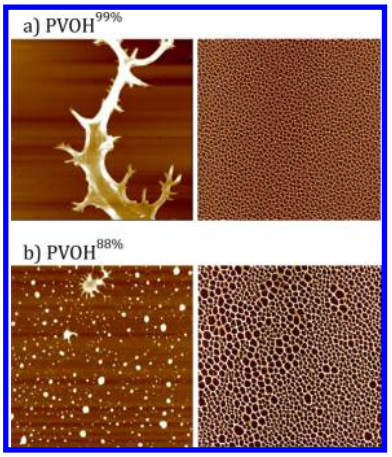


**Figure 8.** AFM images (size, 20 × 20 $\mu m^2$) of $PVOH^{99\%}$ (top) and $PVOH^{88\%}$ (bottom) thin films adsorbed on $PDMS^{49k}$ substrates before (left; height scale, 100 nm) and after (right; height scale, 20 nm) 1 s of oxygen plasma treatment.

which are lower than those of the untreated (109°/95°) but are almost identical to those of the native $PDMS^{2k}$ (101°/79°). The significant change in the PVOH morphology is most likely due to the reduction in the substrate contact angles after plasma treatment. Both types of PVOH thin films exhibit the more continuous honeycomb morphology, which is presumably caused by the pinning of the receding contact line during thin film dewetting. After adsorption with $PVOH^{99\%}$ and $PVOH^{88\%}$, contact angles decreased to 96°/15° and 103°/20°, respectively. They are higher than those on PVOH−$PDMS^{2k}$ (73°/14° and 92°/14°), especially in advancing contact angles. The higher advancing contact angles of PVOH thin films on the treated $PDMS^{49k}$ are attributed to the hydrophobicity of the exposed PDMS substrate. Furthermore, there is little difference in the adsorbed amount on the treated and untreated PDMS substrates. On the lightly plasma-treated $PDMS^{116k}$ substrates, $PVOH^{99\%}$ and $PVOH^{88\%}$ thin films also exhibit primarily the honeycomb morphologies instead of the fractal or droplet morphologies (not shown here). We should point out that plasma treatment not only reduces hydrophobicity of PDMS substrates, but also ultimately results in the formation of a harder, silica-like surface layer.[37−41] Thus, we cannot decouple the effects of surface wettability and liquid-like characteristic on the extent of dewetting. It is also worth noting that it is important to control the extent of substrate oxidation because the adsorbed amount of PVOH is noticeably decreased on more oxidized PDMS substrates where the hydrophobic driving force for adsorption is lessened.

The impact of the light plasma treatment of PDMS substrates on the morphology and wettability of the adsorbed PVOH thin films leads to a practical solution to hydrophilize PDMS substrates via PVOH adsorption. The data presented here demonstrate that the extent of plasma oxidation should be kept low to gain the benefit of pinning PVOH thin films from extensive dewetting without compromising the hydrophobic driving force for adsorption.

Hydrophobic recovery is a main obstacle in hydrophilization of silicones. To assess the stability of the hydrophilized PDMS substrates, wettability of PVOH-adsorbed $PDMS^{2k}$ and plasma-treated $PDMS^{49k}$ samples was monitored for at least 1 week under ambient conditions. The initial contact angle measurements were carried out 24 h after PVOH adsorption to allow


DOI: 10.1021/acs.langmuir.6b00470
Langmuir 2016, 32, 3191−3198

thin films sufficient time to dry. All the samples appeared to maintain their hydrophilicity over time since no detectable change in water contact angles was observed (Figure 5S). We emphasize that hydrophobic recovery is not observed even when PVOH coverage is incomplete on plasma-treated PDMS (Figure 8). This result implies that factors contributing to hydrophobic recovery in typical silicone systems, including low molecular weight silicone species migration to the surface and surface reconstruction,[36−40] are absent here.

## CONCLUSIONS

Poly(dimethylsiloxane) substrates were prepared by grafting linear PDMS polymers of 2, 9, 17, 49, and 116 kDa onto silicon wafers. Adsorption of two types of poly(vinyl alcohol) (PVOH), 99% and 88% hydrolyzed, was carried out on the PDMS substrates in aqueous solution. The PVOH thin film morphologies were found to depend on PDMS molecular weight/thickness as well as PVOH degree of hydrolysis.

As PDMS thickness increases, the adsorbed PVOH becomes progressively unstable and transitions from continuous films on $PDMS^{2k}$, to honeycomb-like, and then to fractal/droplet morphologies on higher molecular weight PDMS substrates. The in situ optical microscopy imaging study revealed that the formation of the discontinuous morphologies takes place upon sample exposure to air. The morphological changes are attributed to the lower receding contact angle of $PDMS^{2k}$ causing pinning of the PVOH films and the more liquid-like characteristic of the thicker PDMS layers rendering instability in the thin films during drying.

The most notable difference between $PVOH^{99\%}$ and $PVOH^{88\%}$ thin films is that the former present in fractal morphologies and the latter manifest as specks on high molecular weight PDMS substrates. Crystallization of $PVOH^{99\%}$ during the dehydration process in a diffusion-limited aggregation fashion is attributed to give rise to the unique fractal features, whereas there is insufficient crystallization driving force in $PVOH^{88\%}$ so that the common droplet morphology is formed. On the basis of this study and those reported in the literature, we hypothesize that crystallization is a necessary driving force for forming fractal morphology during thin film dewetting.

Significantly enhanced hydrophilicity is only realized on $PDMS^{2k}$ with continuous coverage of PVOH films. Light plasma treatment of the higher molecular weight PDMS substrates was carried out to mimic the lower receding contact angle and less liquid-like properties of the $PDMS^{2k}$ substrate. On the treated PDMS substrates, the adsorbed PVOH thin films exhibit the honeycomb morphology instead of the more discontinuous fractal and droplet morphologies on the untreated substrates and enhanced wettability upon PVOH adsorption was accomplished. Hydrophobic recovery of PVOH-adsorbed PDMS substrates was absent during a 1 week period. We have demonstrated that light plasma oxidation and subsequent PVOH adsorption can be utilized as a means to effectively hydrophilize conventional PDMS substrates.

## ASSOCIATED CONTENT

### Supporting Information

The Supporting Information is available free of charge on the ACS Publications website at DOI: 10.1021/acs.langmuir.6b00470.

Optical microscopy time-lapse images, TEM images, and water contact angles of $PVOH^{99\%}$ and $PVOH^{88\%}$ thin films adsorbed on PDMS substrates (PDF)

## AUTHOR INFORMATION


### Corresponding Author

*E-mail: weichen@mtholyoke.edu. Phone: 413-538-2224. Fax: 413-538-2327.

### Author Contributions

†A.K. and L.N. contributed equally to this work.


### Notes

The authors declare no competing financial interest.

## ACKNOWLEDGMENTS

Financial support was provided by the National Science Foundation (DMR-1404668 and DMR-0820506). The authors are grateful to Dr. Alexander Ribbe and Blanca Carbajal Gonzalez for their respective assistance in TEM and in situ optical microscopy work. The use of the NSF-MRSEC central facilities at the University of Massachusetts is also acknowledged.

## REFERENCES


(1) Seyferth, D. Dimethyldichlorosilane and the Direct Synthesis of Methylchlorosilanes. The Key to the Silicones Industry. *Organometallics* **2001**, *20*, 4978−4992.

(2) McGregor, R. R. *Silicones and Their Uses*; McGraw-Hill: NewYork, 1954.

(3) Clarson, S. J.; Semlyen, J. A. *Siloxane Polymers*; Prentice Hall: Englewood Cliffs, NJ, 1993.

(4) Wu, S. In *Polymer Handbook*, 4th ed.; Brandrup, J., Immergut, E. H., Grulke, E. A., Eds.; John Wiley & Sons: New York, 1999; pp VI-231 and VI-524.

(5) Kuo, A. C. M. In *Polymer Data Handbook*; Mark, J. E., Ed.; Oxford University Press: New York, 1999; p 423.

(6) Dvornic, P. R.; Lenz, R. W. *High Temperature Siloxane Elastomers*; Huthig and Wepf: Basel, Switzerland, 1990.

(7) Zhou, J.; Ellis, A. V.; Voelcker, N. H. Recent Developments in PDMS Surface Modification for Microfluidic Devices. *Electrophoresis* **2010**, *31*, 2−16.

(8) Zhou, J.; Khodakov, D. A.; Ellis, A. V.; Voelcker, N. H. Surface Modification for PDMS-based Microfluidic Devices. *Electrophoresis* **2012**, *33*, 89−104.

(9) Wu, D.; Luo, Y.; Zhou, X.; Dai, Z.; Lin, B. Multilayer Poly(vinyl alcohol)-adsorbed Coating on Poly(dimethylsiloxane) Microfluidic Chips for Biopolymer Separation. *Electrophoresis* **2005**, *26*, 211−218.

(10) Carneiro, L. B.; Ferreira, J.; Santos, M. J. L.; Monteiro, J. P.; Girotto, E. M. A New Approach to Immobilize Poly(vinyl alcohol) on Poly(dimethylsiloxane) Resulting in Low Protein Adsorption. *Appl. Surf. Sci.* **2011**, *257*, 10514−10519.

(11) He, T.; Liang, Q.; Zhang, K.; Mu, X.; Luo, T.; Wang, Y.; Luo, G. A Modified Microfluidic Chip for Fabrication of Paclitaxel-loaded Poly(L-lactic acid) Microspheres. *Microfluid. Nanofluid.* **2011**, *10*, 1289−1298.

(12) Yu, L.; Li, C. M.; Zhou, Q.; Luong, J. H. T. Poly(vinyl alcohol) Functionalized Poly(dimethylsiloxane) Solid Surface for Immunoassay. *Bioconjugate Chem.* **2007**, *18*, 281−284.

(13) Coupe, B.; Chen, W. New Approaches to Surface Functionalization of Fluoropolymers. *Macromolecules* **2001**, *34*, 1533−1535.

(14) Chen, W. Surface Modification of Solid Phase Objects by Poly(vinyl alcohol). U.S. Patent 7179506B2, 2007.

(15) Kozlov, M.; Quarmyne, M.; Chen, W.; McCarthy, T. J. Adsorption of Poly(vinyl alcohol) to Hydrophobic Substrates: A General Approach for Hydrophilizing and Chemically Activating Surfaces. *Macromolecules* **2003**, *36*, 6054−6059.




DOI: 10.1021/acs.langmuir.6b00470
*Langmuir* 2016, 32, 3191−3198

(16) Kozlov, M.; McCarthy, T. J. Adsorption of Poly(Vinyl Alcohol) from Water to a Hydrophobic Surface: Effects of Molecular Weight, Degree of Hydrolysis, Salt, and Temperature. *Langmuir* **2004**, *20*, 9170−9176.
(17) Barrett, D. A.; Hartshorne, M. S.; Hussain, M. A.; Shaw, P. N.; Davies, M. C. Resistance to Nonspecific Protein Adsorption by Poly(vinyl alcohol) Thin Films Adsorbed to a Poly(styrene) Support Matrix Studied Using Surface Plasmon Resonance. *Anal. Chem.* **2001**, *73*, 5232−5239.
(18) Serizawa, T.; Hashiguchi, S.; Akashi, M. Stepwise Assembly of Ultrathin Poly(vinyl alcohol) Films on a Gold Substrate by Repetitive Adsorption/Drying Processes. *Langmuir* **1999**, *15*, 5363−5368.
(19) Bunn, C. W. Crystal Structure of Polyvinyl alcohol. *Nature* **1948**, *161*, 929−930.
(20) Seemann, R.; Herminghaus, S.; Jacobs, K. Dewetting Patterns and Molecular Forces: A Reconciliation. *Phys. Rev. Lett.* **2001**, *86*, 5534−5537.
(21) Gentili, D.; Foschi, G.; Valle, F.; Cavallini, M.; Biscarini, F. Applications of Dewetting in Micro and Nanotechnology. *Chem. Soc. Rev.* **2012**, *41*, 4430−4443.
(22) Xue, L.; Han, Y. Pattern Formation by Dewetting of Polymer Thin Film. *Prog. Polym. Sci.* **2011**, *36*, 269−293.
(23) Reiter, G. Dewetting of Thin Polymer Films. *Phys. Rev. Lett.* **1992**, *68*, 75−78.
(24) Witten, T. A.; Sander, L. M. Diffusion-limited Aggregation, a Kinetic Critical Phenomenon. *Phys. Rev. Lett.* **1981**, *47*, 1400−1403.
(25) Witten, T. A.; Sander, L. M. Diffusion-limited Aggregation. *Phys. Rev. B: Condens. Matter Mater. Phys.* **1983**, *27*, 5686−5697.
(26) Meakin, P. Diffusion-controlled Cluster Formation in Two, Three, and Four Dimensions. *Phys. Rev. A: At., Mol., Opt. Phys.* **1983**, *27*, 604−607.
(27) Chen, L.; Xu, J.; Fleming, P.; Holmes, J. D.; Morris, M. A. Dynamic Stable Nanostructured Metal Oxide Fractal Films Grown on Flat Substrates. *J. Phys. Chem. C* **2008**, *112*, 14286−14291.
(28) Haberko, J.; Bernasik, A.; Luzny, W.; Raczkowska, J.; Rysz, J.; Budkowski, A. Dendrites and Pillars in Spin Cast Blends of Polyaniline or Its Oligomeric Analogue. *Synth. Met.* **2010**, *160*, 2459−2466.
(29) Samanta, T.; Mukherjee, M. Effect of Added Salt on Morphology of Ultrathin Polyelectrolyte Films. *Polymer* **2012**, *53*, 5393−5403.
(30) Zhai, X.; Wang, W.; Zhang, G.; He, B. Crystal Pattern Formation and Transitions of PEO Monolayers on Solid Substrates from Nonequilibrium to Near Equilibrium. *Macromolecules* **2006**, *39*, 324−329.
(31) Bi, W.; Teguh, J. S.; Yeow, E. K. L. Visualizing Polymer Crystallization in Ultrathin Layers Using a Single-macromolecule Tracking Method. *Phys. Rev. Lett.* **2009**, *102*, 048302.
(32) Grohens, Y.; Castelein, G.; Carriere, P.; Spevacek, J.; Schultz, J. Multiscale Aggregation of PMMA Stereocomplexes at a Surface: An Atomic Force Microscopy Investigation. *Langmuir* **2001**, *17*, 86−94.
(33) Taguchi, K.; Toda, A.; Miyamoto, Y. Crystal Growth of Isotactic Polystyrene in Ultrathin Films: Thickness and Temperature Dependence. *J. Macromol. Sci., Part B: Phys.* **2006**, *45*, 1141−1147.
(34) Jacquemart, I.; Pamuła, E.; De Cupere, V. M.; Rouxhet, P. G.; Dupont-Gillain, C. C. Nanostructured Collagen Layers Obtained by Adsorption and Drying. *J. Colloid Interface Sci.* **2004**, *278*, 63−70.
(35) Krumpfer, J. W.; McCarthy, T. J. Rediscovering Silicones: "Unreactive" Silicones React with Inorganic Surfaces. *Langmuir* **2011**, *27*, 11514−11519.
(36) Nguyen, L.; Hang, M.; Wang, W.; Tian, Y.; Wang, L.; McCarthy, T. J.; Chen, W. Simple and Improved Approaches to Long-lasting, Hydrophilic Silicones Derived from Commercially Available Precursors. *ACS Appl. Mater. Interfaces* **2014**, *6*, 22876−22883.
(37) Hillborg, H.; Gedde, U. W. Hydrophobic Recovery of Polydimethylsiloxane after Exposure to Corona Discharges. *Polymer* **1998**, *39*, 1991−1998.
(38) Hillborg, H.; Ankner, J. F.; Gedde, U. W.; Smith, G. D.; Yasuda, H. K.; Wikstrom, K. Crosslinked Polydimethylsiloxane Exposed to Oxygen Plasma Studied by Neutron Reflectometry and Other Surface Specific Techniques. *Polymer* **2000**, *41*, 6851−6863.
(39) Hillborg, H.; Sandelin, M.; Gedde, U. W. Hydrophobic Recovery of Polydimethylsiloxane after Exposure to Partial Discharges as a Function of Crosslink Density. *Polymer* **2001**, *42*, 7349−7368.
(40) Kim, J.; Chaudhury, M. K.; Owen, M. J.; Orbeck, T. The Mechanisms of Hydrophobic Recovery of Polydimethylsiloxane Elastomers to Partial Electrical Discharges. *J. Colloid Interface Sci.* **2001**, *244*, 200−207.
(41) Morra, M.; Occhiello, E.; Marola, R.; Garbassi, F.; Humphrey, P.; Johnson, D. On the Aging of Oxygen Plasma-Treated Polydimethylsiloxane Surfaces. *J. Colloid Interface Sci.* **1990**, *137*, 11−24.


DOI: 10.1021/acs.langmuir.6b00470
*Langmuir* 2016, 32, 3191−3198